





Journal Name

COMMUNICATION

## Induced Circular Dichroism of monoatomic anions: Silica-assisted chiral environment transfer from molecular assembled nanohelices to halide ions

Received 00th January 20xx,  
Accepted 00th January 20xx

DOI: 10.1039/x0xx00000x

www.rsc.org/

Yutaka Okazaki,<sup>a</sup> Naoya Ryu,<sup>b</sup> Thierry Buffeteau,<sup>c</sup> Shaheen Pathan,<sup>a,d</sup> Shoji Nagaoka,<sup>b,e</sup> Emilie Pouget,<sup>a</sup> Sylvain Nlate,<sup>a</sup> Hiroataka Ihara<sup>d,e</sup> and Reiko Oda\*<sup>a</sup>

**We demonstrate the first example of induced CD of mono-atomic anions. This was detected using chirally-arranged molecular assemblies of non-chiral cationic gemini surfactants (16-2-16) with monoatomic anions stabilized with silica-coating. Furthermore, we have also achieved multi-step transfer of chiral environment through the *in-situ* chemical reaction *via* the chiralized monoatomic anions.**

Chiral ions have various attractive properties as represented by asymmetric catalytic activity,<sup>1</sup> enantioselectivity,<sup>2</sup> and chiroptical property,<sup>3</sup> because of the chiral perturbation on their environment through the strong electrostatic interaction. Numerous chiral ionic systems, such as ionic molecules,<sup>4</sup> coordination complexes,<sup>5</sup> ionic self-assemblies,<sup>6</sup> and ionic helical polymers,<sup>7</sup> have been reported so far. However, little is yet known about the chiral property of monoatomic anions in contrast to well-studied chiral induction on monoatomic cations.<sup>3b,8</sup> The most commonly encountered problem is the difficulty to detect their chiral signals by conventionally used techniques such as circular dichroism (CD), vibrational CD (VCD), circularly polarized luminescence (CPL) and Raman optical activity (ROA) spectroscopies. Although monoatomic anions are presumed to have a chiral information when they exist as counterions of chiral molecular system, no direct evidence have been shown because their absorption bands (< 220 nm) overlap with the large absorption band of aromatic or carbonyl groups (< 250 nm) which often constitute a part of chiral molecular systems.<sup>4-7</sup> In this paper, the chiral property of

monoatomic halide ions is studied. To carry out this study, chiral molecular assembly system showing no absorption bands in the middle-UV region (200-300 nm) was used as a

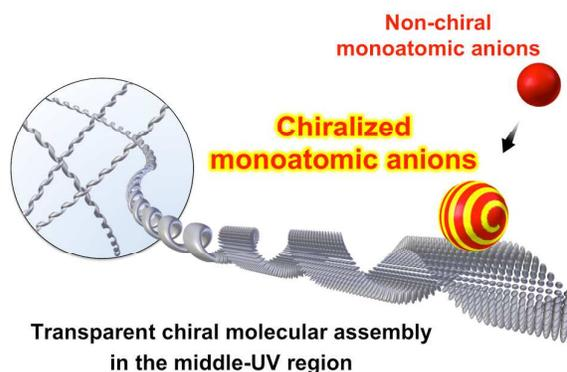


Fig.1 Schematic illustration of how non-chiral monoatomic anions placed in a chiral environment created by molecular assembling system show chiroptical properties.

chiral nano-space providing agent complexed with monoatomic anions (Figure 1). This approach allows us to elucidate the chiroptical properties of halide ions by using conventional CD spectroscopy method. Furthermore, we demonstrate that such a system can serve as a reactor for the multistep chirality induction.

We previously reported the chiral molecular assembly system with the unique properties described as follows: (1) It is based on non-chiral gemini-type dialkyl diammonium amphiphilic molecules that do not have specific absorption band above 200 nm, which self-assemble to form twisted and helical nanoribbons and nanotubes<sup>9</sup> when complexed with chiral tartrate counterion (16-2-16 tartrate). (2) Once they form such chiral double bilayer-based nanostructures, they can go under silica-coating sol-gel transcription procedure with tetraethoxysilane (TEOS), after which original chiral molecular arrangement is maintained in silica even when tartrate, which is the origin of the chirality, is exchanged by other anions.<sup>10</sup> For the present study, we selected such hybrid organic-inorganic structures as chiral nano-space providing agents.

<sup>a</sup> Institute of Chemistry & Biology of Membranes & Nanoobjects (UMR5248 CBMN), CNRS - Université de Bordeaux - Bordeaux INP, 2 rue Robert Escarpit, 33607 Pessac, France

<sup>b</sup> Materials Development Department, Kumamoto Industrial Research Institute, 3-11-38 Higashimachi, Higashi-ku Kumamoto 862-0901, Japan

<sup>c</sup> Institut des Sciences Moléculaires (UMR5255 ISM), CNRS - Université de Bordeaux, 351 Cours de la Libération, 33405 Talence, France

<sup>d</sup> Department of Applied Chemistry and Biochemistry, Kumamoto University, 2-39-1 Kurokami, Chuo-ku Kumamoto 860-8555, Japan

<sup>e</sup> Kumamoto Institute for Photo-Electro Organics (PHOENICS), 3-11-38 Higashimachi, Higashi-ku Kumamoto 862-0901, Japan

Electronic Supplementary Information (ESI) available: Experimental details and supplementary figures. See DOI: 10.1039/x0xx00000x

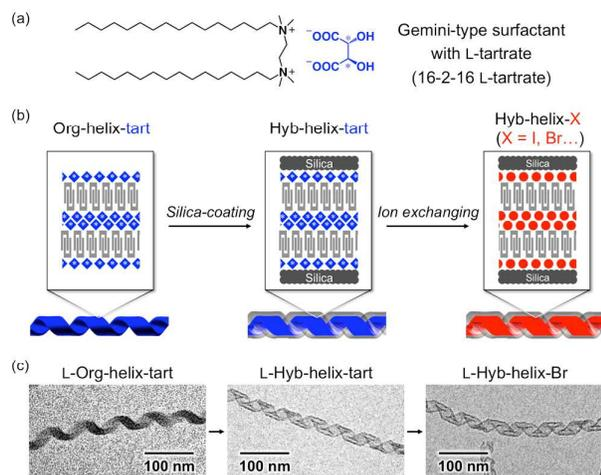


Fig. 2 (a) Chemical structure of 16-2-16 L-tartrate. (b) Preparation scheme of silica-coated organic nanohelices. (c) TEM images of the self-assembly of 16-2-16 L-tartrate, L-Hyb-helix-tart, and L-Hyb-helix-Br from the left to right.

Silica-coated organic self-assembled nanohelices with tartrate (Hyb-helix-tart) were prepared by the procedure described previously (see supporting information).<sup>10,11</sup> Unreacted TEOS was removed by washing with centrifugation with water at 4 °C. Here, it is important to note that 16-2-16 tartrate is not soluble in water at this temperature. Subsequently, it was washed with 100 mM-KX (X = I, Br, Cl, F) aqueous solutions in order to exchange the counterions tartrate by X<sup>-</sup> and to obtain the silica-coated self-assembled nanohelices with halide ions (Hyb-helix-X).

As shown in Figure 2c, the original morphology of self-assembled nanohelices was maintained after silica-coating and washing with water or KBr aqueous solution. *In situ* ion exchanging from tartrate to halide ions in the hybrid silica-organic structure was evaluated by infrared (IR) and <sup>1</sup>H-NMR Spectroscopies. The IR spectrum of the L-Hyb-helix-Br shows the disappearance of the strong absorption peak associated

with antisymmetric ( $\nu_s\text{CO}_2^-$ ) *In situ* ion exchanging from tartrate to halide ions in the hybrid silica-organic structure was evaluated by infrared (IR) and <sup>1</sup>H-NMR spectroscopies. The IR spectrum of the L-Hyb-helix-Br shows stretching mode of the carboxylate groups of the tartrate at 1611 cm<sup>-1</sup>, whereas no significant change was observed in the 3000-2800 cm<sup>-1</sup> region associated with the asymmetric ( $\nu_s\text{CH}_2$ ) and symmetric ( $\nu_s\text{CH}_2$ ) stretching vibrations of the methylene groups from gemini hydrocarbon chains with trans conformations (crystalline-state) (Figure S1). The organic component of silica-coated self-assembled nanohelices was extracted by methanol at 60 °C and evaluated by <sup>1</sup>H-NMR spectral measurements. The extract from the L-Hyb-helix-Br clearly showed peaks corresponding to the 16-2-16 moieties whereas no peak, which corresponds to the protons from the asymmetric carbon of tartrate at 4.36 ppm, was observed (Figure S2). The silica residue contained no carbon element (under the detection limit), as confirmed by elemental analysis (EA) confirming all the organic molecules are extracted in methanol. These results further confirmed that the tartrates were replaced with the bromide ions by the washing with KBr solution. To quantify the organic component of silica-coated self-assembled nanohelices, thermal gravimetric analysis (TGA) was performed. The L-Hyb-helix-tart and the L-Hyb-helix-Br shows 29.4 wt% and 30.0 wt% weight loss respectively upon heating at around 500 °C (Figure S3). These values are very close to the estimated weight of organic gemini (30.7 wt%, see supporting information) expected to create the hybrid structure originally. Thus, we conclude that quasi-totality of the 16-2-16 molecular assemblies remained in the silica walls after washing with water and KBr aqueous solution.

The chiral information of silica-coated self-assembled nanohelices was evaluated by CD spectral measurements. The L- (and D-) Hyb-helix-tart shows clear split Cotton effects at the absorption band below 240 nm (Figures 3a,b).

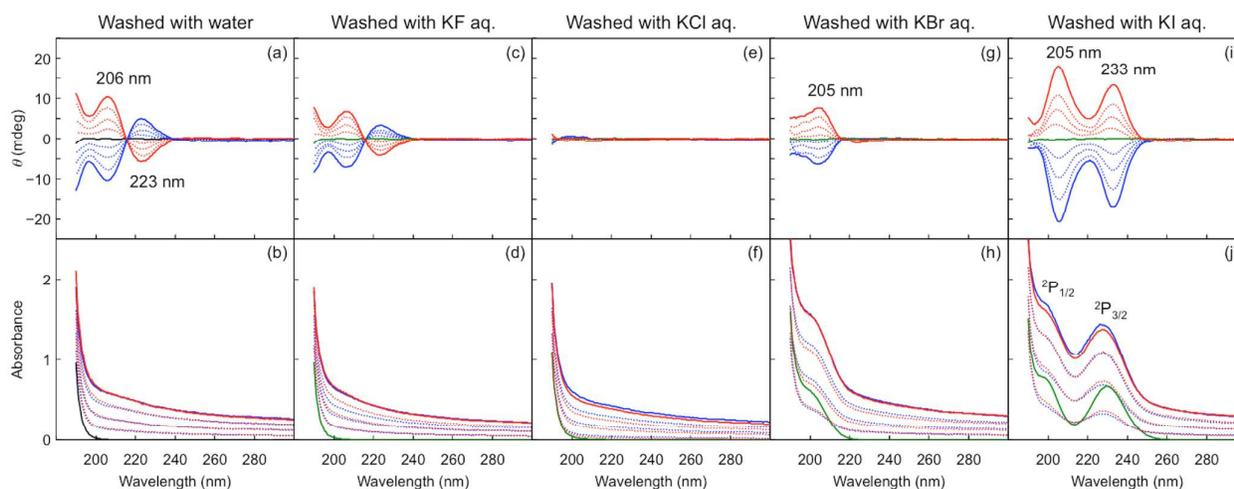


Fig. 3 CD and UV-vis absorbance spectra of various L- (red) and D- (blue lines) silica-coated self-assembled nanohelices in water (0.05-0.20 mg mL<sup>-1</sup>) obtained by washing with (a,b) water, (c,d) 100 mM-KF, (e,f) 100 mM-KCl, (g,h) 100 mM-KBr, and (i,j) 100 mM-KI aqueous solutions, respectively. Black and green spectra represent water (b) and 0.05 mM-KX (X = F, (b); Cl, (f); Br, (h); I, (j)) aqueous solutions, respectively.

This spectral pattern was quite similar to the CD signals from the carboxylates of tartrate, which assembles with 16-2-16 into chiral bilayer (Figure S4).<sup>12</sup> Based on these results, it is considered that chiral organization of tartrate and 16-2-16 surfactants were maintained even after silica-coating. Surprisingly, the L-Hyb-helix-Br shows the remarkable positive Cotton effect at the charge-transfer-to-solvent (CTTS) transition band of hydrated bromide<sup>13</sup> (around  $\lambda_{\text{max}} = 205 \text{ nm}$ ) with a disappearance of CD peak at 223 nm corresponding to the absorption of tartrate (Figures 3g,h). When the Hyb-helix-tart was washed with KI aqueous solution, large Cotton effects were observed at 233nm and 205 nm corresponding to the CTTS transition from hydrated iodide to water ( $^2P_{3/2}$  and  $^2P_{1/2}$ )<sup>13</sup> (Figures 3i,j). For both cases, opposite signals were obtained from D-Hyb-helix-Br and -, respectively. Since both bromide and iodide ions are non-chiral, it is evident that these CD signals are due to the chiral induction from silica-coated self-assembled nanohelices. To our best knowledge, this is the first time that CD signals of monoatomic anions were directly detected. In the case of chloride ion, no Cotton effect was observed at above 200 nm. This is coherent with the fact that the CTTS bands of chloride is at lower wavelength (around  $\lambda_{\text{max}} = 180 \text{ nm}$ )<sup>13</sup> (Figures 3e,f). It also confirms the complete ion exchange from tartrate to chloride ions. On the other hand, no modification on the CD patterns were observed when of L- and D-helix-tart were washed with KF aqueous solution except for a small intensity decrease (Figures 3c, d). It is suggested that tartrates were maintained even after washing with KF solution. IR spectra of these silica-coated self-assembled nanohelices strongly support this idea (Figure S5). This can be explained by the difference in the cation-anion interaction following the Hofmeister effect, which is represented by hydration free energy of the anions<sup>14</sup>,  $\text{N-F} < \text{N-tart} < \text{N-Cl} < \text{N-Br} < \text{N-I}$ .

To understand how these halide ions show CD signals, temperature dependence of L-Hyb-helix-I was studied by CD, UV and IR absorption spectral changes in the heating process. As shown in figures 4a,c, positive Cotton effects were observed at 233 nm and 205 nm at below 30 °C ( $T_{C1}$ ). Upon heating, no significant changes were observed in the helical morphology of silica (Figure 4e) and the crystallinity of alkyl chains up to 45 °C (Figures S6). However, a considerable decrease of UV absorption of  $^2P_{3/2}$  band was observed and the Cotton effects disappeared. They were not recovered after cooling the solution back at 20 °C (Figure 4c,d, S7). These results indicate that the CD signal of the halide ions is induced from chiral arrangement of 16-2-16 surfactants (chiral crystalline state), which is formed with tartrate before ion exchanging and memorized by silica-coating. Further heating above 50 °C ( $T_{C2}$ ) leads to a noticeable increase of  $^2P_{3/2}$  absorption, which indicates the increased number of hydration water molecules.<sup>13</sup> IR spectra show drastic peak shifts of  $\nu_s\text{CH}_2$  (2924  $\text{cm}^{-1}$ ) and  $\nu_s\text{CH}_2$  (2854  $\text{cm}^{-1}$ ), indicating a phase transition of alkyl chain from crystalline to melted state. These results suggest that the trapped iodide ions in the silica-walls were released by melting of alkyl chain of 16-2-16 surfactants. The TEM images of the sample at this temperature show that silica

helices are destroyed (Figure 4e). This is probably due to the high local acidity.

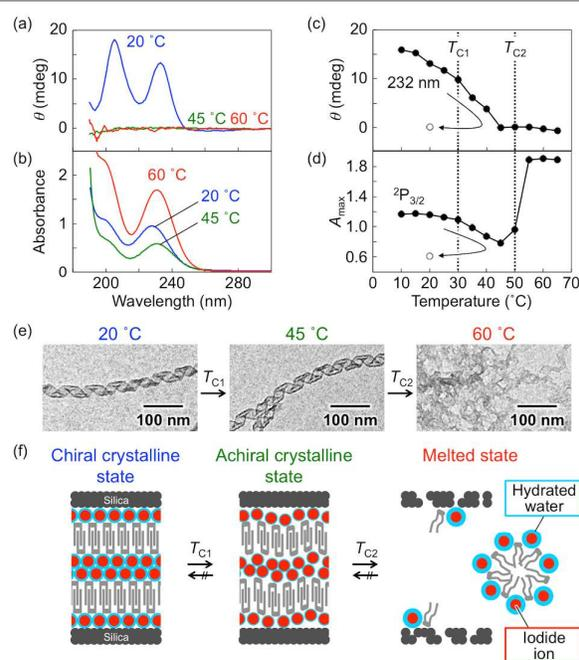


Fig. 4 (a) CD and (b) UV absorbance spectra of L-Hyb-helix-I in water at 20, 45, and 60 °C. Temperature dependence of (c) ellipticities at 232 nm, (d) UV absorbance of  $^2P_{3/2}$  band. (e) TEM images of the dried samples of L-Hyb-helix-I in water at 20, 45 and 60 °C. (f) Schematic illustration of phase transition behavior of L-Hyb-helix-I in aqueous solution.

The induced CD (ICD) of halide ions can originate from two possible mechanisms: (1) symmetry breaking of electron orbital of monomeric halide ion, or (2) exciton coupling from chiral organization of halide ions. The effect of added KI to L-Hyb-helix-Cl and the resulting *in-situ* ion exchange was monitored by CD and UV measurements (Figure S9). UV absorption bands of  $^2P_{1/2}$  and  $^2P_{3/2}$  of iodide increased almost linearly upon KI addition, indicating that the chloride ions progressively exchanged by iodide ions. CD peaks at the absorption bands of  $^2P_{1/2}$  and  $^2P_{3/2}$  of iodide also increased linearly until it reached to plateau. If the CD signals are derived from exciton coupling, we should expect a threshold concentration of iodide ions below which no CD would be observed. In addition, no significant peaks shift was observed between free and incorporated iodide in the hybrid helix system. Therefore, the ICD of iodide is probably originated from symmetry breaking of electron orbital of monomeric halide ions.

We have then demonstrated that such hybrid chiral structure can be used for further chirality induction. First example was observed with the oxidation of  $\text{I}^-$  by adding  $\text{H}_2\text{O}_2$  in the L- (or D-) Hyb-helix-I aqueous solution. As shown in Figure 5a, the Cotton effects ( $|g_{\text{CD}}| = 4 \times 10^{-4}$  at 398 nm) were observed at a newly appeared absorption peak attributed to the  $\text{I}_2$  molecules. Second example is observed in the production of metal halide. It is well known that  $\text{CuI}$  and  $\text{I}_2$  are produced by mixing  $\text{CuSO}_4$  and KI in water. When the L- (or D-)

Hyb-helix-I was added into  $\text{CuSO}_4$  aqueous solution, no significant peak was observed in the UV-visible absorption spectrum (Figure S10). After addition of the KI aqueous solution, new peaks (around 290 nm and 360 nm) appeared accompanied with positive (or negative) Cotton effects (Figure 5b, green line). These results indicate that the L- (and D-) Hyb-helix-I provided a chiral environment upon formation of  $\text{CuI}$  and  $\text{I}_2$ . Given the similar  $|g_{\text{CD}}|$ s before and after the reaction from  $\text{I}^-$  ( $|g_{\text{CD}}| = 5 \times 10^{-4}$  at 207 nm and  $4 \times 10^{-4}$  at 235 nm) to  $\text{CuI}/\text{I}_2$  ( $|g_{\text{CD}}| = 5 \times 10^{-4}$  at 318 nm and  $3 \cdot 4 \times 10^{-4}$  at around 400 nm), we can conclude that there is almost no chirality loss during the transformation from  $\text{I}^-$  to  $\text{CuI}$  and  $\text{I}_2$ . Furthermore, when the L- (and D-) Hyb-helix-CuI are excited at 290 nm, yellow colored luminescence were observed with CPL signals ( $|g_{\text{lum}}| = 2 \times 10^{-4}$  at 550 nm) (Figure 5b, red line).

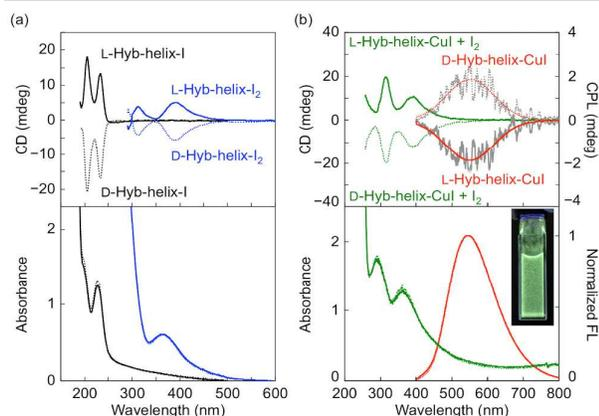


Fig. 5 (a) CD and UV-vis spectra of L- and D-Hyb-helix-I in water before (black) and after (blue) adding  $\text{H}_2\text{O}_2$  aqueous solution. (b) CD and UV-Vis spectra of  $\text{CuSO}_4$  aqueous solutions after adding KI aqueous solution in the presence of L- and D-Hyb-helix-I (green line). CPL and fluorescence spectra of  $\text{CuI}$  with L- and D-Hyb-helix-I (red line). The ex. wavelength was  $\lambda = 290$  nm. The inset image shows L-Hyb-helix-CuI in water under UV light.

In conclusion, we have reported the first example of ICD of monoatomic anions. Such chiral signals of monoatomic anions could be detected using silica-coated chiral molecular assembly from non-chiral gemini-type surfactant that do not have specific absorption band above 200 nm. On the basis of temperature dependence study, it is demonstrated that the ICD of monoatomic anions originates from the memorized chiral organization of 16-2-16 surfactants. Such system could be used as a very promising chiral nano-reactor through multistep chiral induction.

This work was supported by the Strategic International Collaborative Research Program between JST in Japan and ANR in France, and France-Japan International Associated Laboratory on Chiral Nanostructures for Photonic Applications (LIA-CNPA). T.B., E.P., S.N., and R.O. thank the Centre national de la recherche scientifique and Université de Bordeaux. Y.O. thanks the JSPS Overseas Research Fellowship supported by the Japan Society for the Promotion of Science.

## Conflicts of interest

There are no conflicts to declare.

## Notes and references

- (a) R. Noyori and H. Takaya, *Acc. Chem. Res.* 1990, **23**, 345; (b) T. Ooi and K. Maruoka, *Angew. Chem. Int. Ed.* 2007, **46**, 4222; (c) K. Brak and E. N. Jacobsen, *Angew. Chem. Int. Ed.* 2013, **52**, 534.
- (a) J. J. Bodwin, A. D. Cutland, R. G. Malkani and V. L. Pecoraro, *Coord. Chem. Rev.* 2001, **216–217**, 489; (b) N. M. Maier and W. Lindner, *Anal. Bioanal. Chem.* 2007, **389**, 377.
- (a) Z. Dai, J. Lee and W. Zhang, *Molecules* 2012, **17**, 1247; (b) M. C. Heffern, L. M. Matosziuk, T. J. Meade, *Chem. Rev.* 2014.
- (a) T. Payagala and D. W. Armstrong, *Chirality*, 2012, **24**, 17; (b) D. Parmar, E. Sugino, S. Raja, and M. Rueping, *Chem. Rev.* 2014, **114**, 9047.
- (a) L. Ma, J. M. Falkowski, C. Abney, and W. Lin, *Nat. Chem.* 2010, **2**, 838; (b) J. Crassous, *Chem. Commun.* 2012, 48, 9684.
- (a) P. Terech and R. G. Weiss, *Chem. Rev.* 1997, **97**, 3133; (b) H. Ihara, M. Takafuji and T. Sakurai, in *Encyclopedia of Nanoscience & Nanotechnology*, Ed. H. S. Nalwa, American Scientific Publishers, California, 2004, Vol. 9, pp. 473–495; (c) H. Cui, M. J. Webber and S. I. Stupp, *Biopolymers*, 2010, **94**, 1; (d) M. Liu, L. Zhang and T. Wang, *Chem. Rev.* 2015, **115**, 7304; (e) E. Yashima, N. Ousaka, D. Taura, K. Shimomura, T. Ikai and K. Maeda, *Chem. Rev.* 2016, **116**, 13752.
- (a) T. Nakano and Y. Okamoto, *Chem. Rev.* 2001, **101**, 4013; (b) E. Yashima, K. Maeda, H. Iida, Y. Furusho and K. Nagai, *Chem. Rev.* 2009, **109**, 6102.
- (a) E. Graf, R. Graff, M. W. Hosseini, C. Huguenard and F. Taulelle, *Chem. Commun.* 1997, 1459; (b) K. Bartik, M. E. Haouaj, M. Luhmer, A. Collet and J. Reisse, *ChemPhysChem* 2000, **1**, 221.
- (a) R. Oda, I. Huc and S. J. Candau, *Angew. Chem. Int. Ed.* 1998, **37**, 2689; (b) R. Oda, I. Huc, M. Schmuts, S. J. Candau and F. C. MacKintosh, *Nature* 1999, **399**, 566; (c) R. Oda, F. Artzner, M. Laguerre and I. Huc, *J. Am. Chem. Soc.* 2008, **130**, 14705.
- N. Ryu, Y. Okazaki, K. Hirai, M. Takafuji, S. Nagaoka, E. Pouget, H. Ihara and R. Oda, *Chem. Commun.* 2016, **52**, 5800.
- (a) T. Delclos, C. Aimé, E. Pouget, A. Brizard, I. Huc, M.-H. Delville and R. Oda, *Nano Lett.* 2008, **8**, 1929; (b) Y. Okazaki, J. Cheng, D. Dedovets, G. Kemper, M.-H. Delville, M.-C. Durrieu, H. Ihara, M. Takafuji, E. Pouget and R. Oda, *ACS Nano* 2014, **8**, 6863; (c) Y. Okazaki, T. Buffeteau E. Suardyban, D. Talaga, N. Ryu, R. Yagi, E. Pouget, M. Takafuji, H. Ihara and R. Oda, *Nano Lett.* 2016, **16**, 6411.
- A. Brizard, D. Berthier, C. Aimé, T. Buffeteau, D. Cavagnat, L. Ducasse, I. Huc and R. Oda, *Chirality*, 2009, **21**, e153.
- (a) E. Rabinowitch, *Rev. Mod. Phys.* 1942, **14**, 112; (b) M. J. Blandamer and M. F. Fox, *Chem. Rev.* 1970, **70**, 59; (c) W. Sheu and Y. Liu, *Chem. Phys.* 2003, **374**, 620; (d) H. Okuyama, Y. Suzuki, S. Karashima, T. Suzuki, *J. Chem. Phys.* 2016, **145**, 074502-1; (e) M. Chiou and W. Sheu, *Int. J. Quantum Chem.* 2017, **117**, e25404.
- S. Manet, Y. Karpichev D. Bassani, R. Kiagus-Ahmad, R. Oda, *Langmuir* 2010, **26**, 10645.